Physics Letters B 806 (2020) 135524

Contents lists available at ScienceDirect

Physics Letters B

www.elsevier.com/locate/physletb

# New magicity $N = 32$ and 34 due to strong couplings between Dirac inversion partners

Jia Liu [a], Yi Fei Niu [a], Wen Hui Long [a,b,*]

[a] School of Nuclear Science and Technology, Lanzhou University, Lanzhou 730000, China
[b] Key Laboratory of Special Function Materials and Structure Design, Ministry of Education, Lanzhou 730000, China

ARTICLE INFO

*Article history:*
Received 4 September 2019
Received in revised form 15 March 2020
Accepted 26 May 2020
Available online 28 May 2020
Editor: J.-P. Blaizot

*Keywords:*
New magicity
Relativistic Hartree-Fock
Dirac spinor

ABSTRACT

The novel nuclear structure in neutron-rich nuclei — the new magicity $N = 32$ and 34 has been confirmed by the intensive experiment measurements (F. Wienholtz et al. (2013) [17]; D. Steppenbeck et al. (2013) [22]; S. Michimasa et al. (2018) [28]; etc.). However, the underlying mechanism of the new magicity is still under discussion. In this letter, we present a new mechanism that the strong couplings between the $s_{1/2}$ (including both neutron and proton ones with different principle numbers) and neutron ($\nu$) $\nu 2p_{1/2}$ orbits, referred as "Dirac inversion partners" (DIPs) which are of the same total angular momentums but opposite parity, play a key role in opening both subshells at $N = 32$ and 34. Such strong couplings originate from the inversion similarity between the DIPs, that the upper component of the Dirac spinor of one partner shares the same angular momentum as the lower component of the other, and vice versa. Following the revealed mechanism, it is predicted that on the proton deficient side ($Z \leqslant 20$) the magicity $N = 32$ is reserved from $^{52}$Ca until $^{48}$S, but vanishes in $^{46}$Si.



Atomic nuclei, composed of protons and neutrons, are self-bound quantum many-body system and exhibit typically different magic shells from atoms due to the strong spin-orbital couplings [1,2]. With the worldwide development of radioactive ion beam facilities and detectors, the research area of nuclear physics is largely extended from the stable nuclei to the ones far from the stability, namely the exotic nuclei. Along the extension from the stable to unstable regions, nuclear shell structure can be systematically or even dramatically changed [3,4], such as the vanishing of the traditional magicity $N = 8$ and 20 in neutron-rich $^{11}$Li [5] and $^{32}$Mg [6], respectively. On the other hand, new magicity can also arise, for instance the $N = 16$ in drip-line magic nucleus $^{24}$O [7–10], which has been reviewed in Ref. [11].

In recent years, intensive interests have been attracted on the occurrences of new magicity $N = 32$ and 34 in neutron-rich $pf$-shell nuclei. Experimentally, the magic nature at $N = 32$ has been manifested by the enhanced $2_1^+$ excitation energy and relatively reduced $B(E2; 0^+ \to 2_1^+)$ transition probabilities in Ar, Ca, Ti and Cr isotopes [12–16], and further confirmed by the high-precision mass measurements of exotic Ca and K isotopes [17–19]. More recently, a strong subshell closure at $N = 32$ was also indicated in Sc isotopes through the direct mass measurement, which is found to be quenched in V isotopes [20,21]. For the magic nature at $N = 34$, it was revealed from the large excitation energy of the $2_1^+$ state (2043 keV) in $^{54}$Ca [22].

Theoretically, the large scale shell model calculations with the GXPF1 and KB3G Hamiltonians reproduce the enhanced $2_1^+$ energies at $N = 32$ [13,23]. Afterwards, the calculations with a beyond-mean-field theory of new generation [24] and the *ab-initio* ones [25] also support the opening of the $N = 32$ subshell in Ca isotopes. However, the theoretical discrepancy was commonly found in describing the magic nature at $N = 34$, in contrast to the one at $N = 32$. For instance, the shell-model calculations using the modified GXPF1 interaction (GXPF1A) give a large gap between $\nu 1f_{5/2}$ and $\nu 2p_{1/2}$ orbits in $^{54}$Ca, i.e., the $N = 34$ subshell [26], while it is not supported by the KB3G interaction [13]. Such discrepancy also exists in the *ab-initio* calculations. It was pointed out in Ref. [27] that an initial three-body force is necessary to reproduce the shell closures in $^{48,52,54}$Ca, while a weak shell effect at $N = 34$ was presented by the *ab-initio* calculations in Ref. [25]. In fact, due to the theoretical discrepancy, one can not help suspecting the robustness of the magic nature at $N = 34$.

Until very recently, the first direct mass measurements of $^{55-57}$Ca provide crucial direct evidence for the magicity $N = 34$ in $^{54}$Ca [28]. It is also worthwhile to mention that the measured $\gamma$-ray spectroscopy of $^{52}$Ar$_{34}$ shows a similar $2_1^+$ energy [1656(18) keV] to that of $^{46}$Ar$_{28}$ [1554(1) keV] [29], an experimental signature of the persistence of the magicity $N = 34$ on the proton-

* Corresponding author.
*E-mail address:* longwh@lzu.edu.cn (W.H. Long).

https://doi.org/10.1016/j.physletb.2020.135524

deficient side ($Z < 20$). These recent experiments make the magicity $N = 34$ as robust as the $N = 32$ one indeed. Thus, it becomes a challenging task for the theorists to provide an unified interpretation on the successive new magicity $N = 32$ and 34, particularly the underlying physics.

Aiming at that, we performed the investigations under the relativistic Hartree and Hartree-Fock approaches [30,31], respectively the relativistic mean field (RMF) and relativistic Hartree-Fock (RHF) models, which own the advantage in deducing the strong spin-orbital coupling self-consistently. Both RMF and RHF approaches are very successful in describing various nuclear phenomena [4,32–41]. However specialized to the magic nature at $N = 32$ and 34 in Ca isotopes, it is not supported by the popular relativistic Lagrangians, such as the RMF ones DD-ME2 [42], PC-PK1 [43] and PK series [44], and the RHF PKO*i* ($i = 1, 2, 3$) [45,46]. In contrast to that, the RHF Lagrangian PKA1 [47], that contains the degree of freedom of the $\rho$-tensor coupling, improves systematically the description of the nuclear structural properties [38,39,48]. More significantly, PKA1 presents prominent subshells at both $N = 32$ and 34 for Ca isotopes [40]. This motivates us to clarify the underlying mechanism from the relativistic point of view, as well as the persistent limit of the magicity $N = 32$.

In this letter, we study the new magicity $N = 32$ and 34 in Ca isotopes by using PKA1 [47], in comparison with PKO3 [46] and DD-ME2 [42]. For all the calculations with selected Lagrangians, the pairing correlations are considered within the BCS scheme by taking the finite-range Gogny force D1S [49] as the pairing force. For the isotopes with odd neutron numbers, the blocking effects have been taken into account in the BCS pairing. It shall be remarked that similar results are obtained by the relativistic Hartree-Fock-Bogoliubov theory [50]. However, it is more straightforward to clarify the mechanism of new magicity under the RHF plus BCS scheme. Besides, the effects of deformation are not considered since most of the concerned nuclei are spherical [51].

Fig. 1 (a) shows the two-neutron separation energies $S_{2n}$ (MeV) calculated by PKA1, PKO3 and DD-ME2, as compared to the experimental data [52] and very recent measurements [28]. Obviously, all the selected models can properly reproduce the trend of $S_{2n}$ from $N = 28$ to 32, and PKA1 presents nice agreement with the data. After the terrace at $N = 30 \sim 32$, a significant descending from $N = 32$ to 36, similar to that from $N = 28$ to 30, is found in the experimental data, a direct evidence of the successive magicity $N = 32$ and 34. Theoretically, the $S_{2n}$ values given by PKO3 and DD-ME2 decrease from $N = 30$ smoothly across $N = 32$ and 34, showing no signal of any shell occurrence. On the contrary, PKA1 properly reproduces the sudden drop at $N = 32$ and such drop continues until $N = 36$, after which a terrace appears. Although the $S_{2n}$ values are systematically overestimated, the near parallel trend with the data still proves that PKA1 provides an appropriate description of the successive magicity $N = 32$ and 34.

From the differences of $S_{2n}$ values of neighboring isotopes, namely the filtering function $\delta e = S_{2n}(N) - S_{2n}(N+1)$ and the two-neutron gap $\Delta_{2n} = S_{2n}(N) - S_{2n}(N+2)$, one can quantify the magicity to certain extent [53]. Figs. 1 (b) and (c) show the $\delta_e$ and $\Delta_{2n}$ values, respectively. Similar as the $S_{2n}$ values, all the selected Lagrangians can properly reproduce both trends of the $\delta e$ and $\Delta_{2n}$ values from $N = 28$ to 30, while these values at $N = 32$ and 34 are underestimated strikingly by PKO3 and DD-ME2. In contrast to that, nice agreements with the data at both $N = 32$ and 34 are obtained by PKA1, which further prove the reliability of the model in describing the new magicity $N = 32$ and 34.

To clarify the mechanism related to the successive magicity $N = 32$ and 34, Fig. 2 shows schematically the 3D plots of both neutron and proton densities (left panels) of $^{52,54}$Ca and the neutron ($\nu$) single-particle (s.p.) energies $\varepsilon_{\nu nlj}$ (right panels), using the RHF Lagrangian PKA1. At first, let's focus on the first two rows in Fig. 2. It is seen that both neutron and proton densities of $^{52}$Ca show distinct central-bumped structures, being consistent with the large spin-orbit (SO) splitting of $\nu 2p$ orbits that gives the $N = 32$ subshell. This can be interpreted well by the mechanism revealed in Refs. [54–57] that the central-bumped or central-depressed density profiles can essentially enlarge or reduce the SO splitting of low-$l$ orbits, such as $p$ states whose probability densities locate at the center of nucleus since the centrifugal repulsion is fairly weak.

While for $^{54}$Ca (the second row in Fig. 2), the neutron density profile becomes even central-depressed, showing a semi-bubble-like structure, and compared to $^{52}$Ca the central-bumped structure vanishes completely in the proton density. Being consistent with the mechanism mentioned above, the $\nu 2p$ splitting is notably reduced in $^{54}$Ca. Meanwhile, such dramatic changes of the central densities show little effect on the $\nu 1f$ splitting, since their probability densities are far away from the interior region due to the strong centrifugal repulsion. Eventually both lead to the occurrence of the $N = 34$ subshell in $^{54}$Ca. From the first two rows of Fig. 2, one can understand the consistent relation between the evolutions of the matter densities and s.p. levels. However, one can't help to ask how the densities can be changed dramatically from the central-bumped structures in $^{52}$Ca to an even central-depressed one in $^{54}$Ca, with only two more neutrons occupying the $\nu 2p_{1/2}$ orbit.

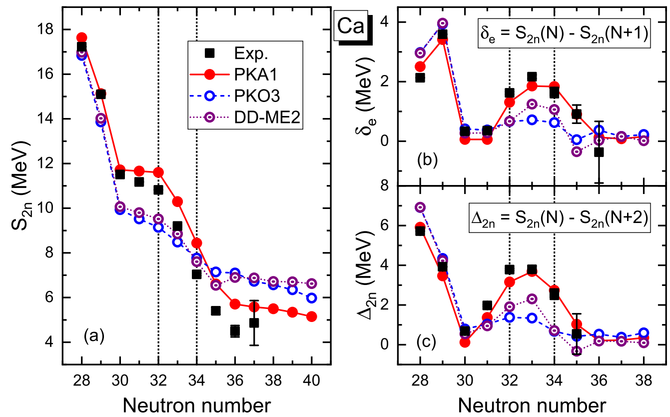


**Fig. 1.** Plot (a) shows two-neutron separation energies $S_{2n}$ (MeV) of Ca isotopes, and plots (b) and (c) for the differences, respectively $\delta e = S_{2n}(N) - S_{2n}(N+1)$ and $\Delta_{2n} = S_{2n}(N) - S_{2n}(N+2)$. The results are calculated by PKA1 [47], PKO3 [46] and DD-ME2 [42], as compared to the data [28,52].

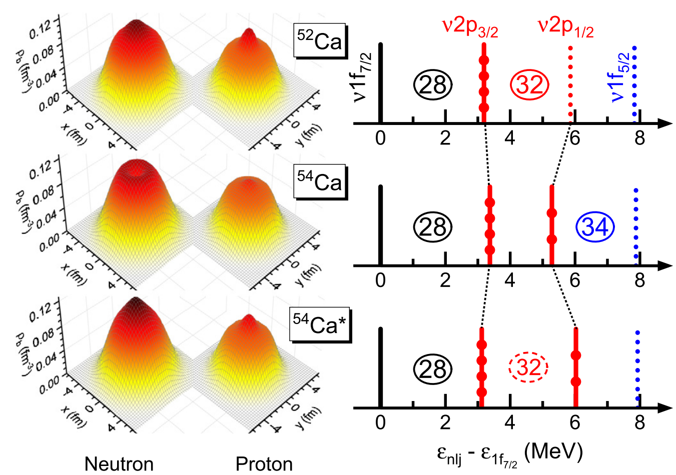


**Fig. 2.** Neutron/proton densities (left panels) and neutron ($\nu$) single-particle levels (right panels) for $^{52,54}$Ca, calculated by PKA1. For the illustration, the last row shows the calculation for $^{54}$Ca that drops the $UL$-terms felt by the $s$-orbits from the DIP $\nu 2p_{1/2}$.

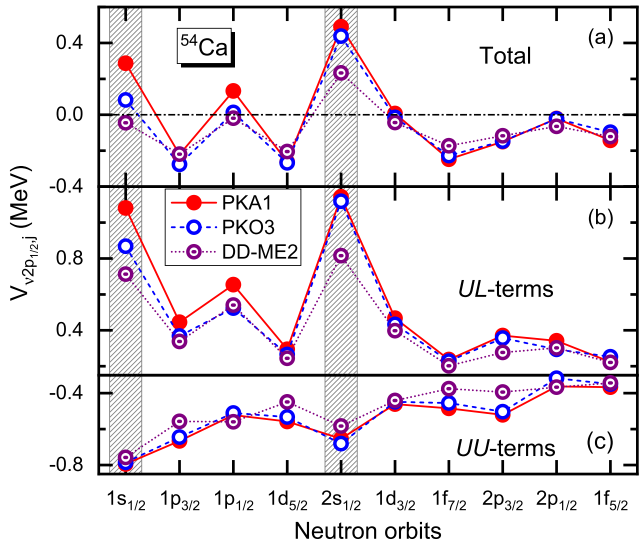


**Fig. 3.** Interacting matrix elements [plot (a)] between the valence neutron $\nu 2p_{1/2}$ orbit and the neutron ones, namely $V_{\nu 2p_{1/2},j}$ (MeV), and the contributions from the $UL$- [plot (b)] and $UU$-terms [plot (c)]. The results are calculated by PKA1, PKO3 and DD-ME2. See the text for details.

For further verification, we show the interaction matrix elements between the $\nu 2p_{1/2}$ orbit and the others in Fig. 3 (a), namely $V_{2p_{1/2},j} = \bar{v}_{l_1 l_2, l_3 l_4}$ with $l_1 = l_3 = \nu 2p_{1/2}$ and $l_2 = l_4 = j$. It is interesting to see that the couplings between the $\nu 2p_{1/2}$ and $s$-orbits (emphasized by shadowed area) are repulsive in general, and PKA1 presents the strongest repulsive results. Since from $^{52}$Ca to $^{54}$Ca two extra neutrons occupy the $\nu 2p_{1/2}$ orbit, such strong repulsion can drive the $s$-orbital neutrons away from the center, as well as the $s$-orbital protons because of the neutron-proton correlations. Namely as compared to $^{52}$Ca, the central probability densities of the $s$-orbits in $^{54}$Ca are reduced, instead of bringing down the occupations of the $s$-orbits. Such variations of the $s$-orbits eventually lead to the central-depressed density profiles from $^{52}$Ca to $^{54}$Ca, seeing Fig. 2.

Under the relativistic scheme, e.g., the RMF and RHF approaches, the Dirac spinors of nucleons contain the upper ($U$) and lower ($L$) components. We notice that the $L$-components of Dirac spinors of the $p_{1/2}$ orbits share the same angular wave functions with the $U$-ones of the $s_{1/2}$ orbits, and vice versa. Here we call such doublet as the “Dirac inversion partners” (DIPs), which are of the same total angular momentum but opposite parity. To understand the repulsive couplings between the DIPs, here $(\nu 2p_{1/2}, \nu s_{1/2})$, we decompose the total interaction matrix elements $V_{2p_{1/2},j}$ [in Fig. 3 (a)] into two parts, the $UL$-terms and $UU$-terms as shown in Figs. 3 (b) and (c), respectively. For the $UU$-term, it contains the contributions only from the $U$-components of Dirac spinors, while the $L$-components contribute the $UL$-terms, namely the ones which exclude the $UU$-terms from the total. Since the $L$-components present tiny contributions to the probability densities, one would not expect substantial contributions from the $UL$-terms to the interaction matrix elements.

However, from Fig. 3 (b) it can be seen that the $UL$-terms are in general repulsive. Such feature can be qualitatively interpreted by the nature of the coupling channels. As an example, Table 1 shows the contributions from the Hartree (H) and Fock (F) terms of various meson-nucleon couplings to the interaction matrix element $V_{\nu 2p_{1/2},\nu 1s_{1/2}}$ (MeV), including the $UU$-, $UL$-terms and the total ($V$). Under the relativistic scheme, e.g., in RMF, the isoscalar $\sigma$-scalar ($\sigma$-S) and $\omega$-vector ($\omega$-V) couplings dominate the nuclear attraction and repulsion, respectively, and cancel with each another to provide residual attraction, seeing the $UU$-H and $V$-H terms in Table 1. In spite of that, for the $UL$-terms, the $\sigma$-S coupling contributes repulsively as the $\omega$-V one, other than counteracting each another, seeing $UL$-H terms in Table 1. It is not difficult to understand from the forms of nuclear scalar and vector densities [4]. It shall be emphasized that not only for the neutron-neutron or proton-proton couplings, the $UL$-terms of the neutron-proton couplings are also repulsive, since they are also dominated by the $\sigma$-S and $\omega$-V couplings.

**Table 1**
Contributions from the Hartree (H) and Fock (F) terms of the $\sigma$-scalar ($\sigma$-S), $\omega$-vector ($\omega$-V), $\rho$-vector ($\rho$-V), $\rho$-tensor ($\rho$-T), $\rho$-vector-tensor ($\rho$-VT) and $\pi$-pseudo-vector ($\pi$-PV) couplings to the interaction matrix element $V_{\nu 2p_{1/2},\nu 1s_{1/2}}$ (MeV), including the $UU$-, $UL$-terms and the total ($V$). The results are calculated by PKA1.

| | $\sigma$-S | $\omega$-V | $\rho$-V | $\rho$-T | $\rho$-VT | $\pi$-PV |
|---|---|---|---|---|---|---|
| $UU$-H | −3.935 | 2.894 | 0.101 | – | – | – |
| $UU$-F | 1.617 | −1.328 | −0.046 | −0.089 | – | −0.007 |
| $UL$-H | 0.359 | 0.269 | 0.009 | 0.000 | 0.001 | – |
| $UL$-F | 0.027 | 0.368 | 0.013 | 0.006 | 0.030 | −0.001 |
| $V$-H | −3.576 | 3.163 | 0.110 | 0.000 | 0.001 | – |
| $V$-F | 1.645 | −0.961 | −0.033 | −0.084 | 0.030 | −0.008 |

Compared to the ordinary cases, the repulsive $UL$-terms are strongly enhanced for the DIPs $(\nu 2p_{1/2}, s_{1/2})$, which lead to strong repulsion between the neutron DIPs, although cancelled partly by attractive $UU$-terms in Fig. 3 (c). Such enhancement can be understood well from the inversion similarity between the DIPs, i.e., the $U$-/$L$-components of $\nu 2p_{1/2}$ orbit and the $L$-/$U$-ones of its DIPs $s_{1/2}$ share the same angular momentum. Implemented with the Fock terms, namely the RHF approach, the space parts of the vector couplings ($\omega$-V and $\rho$-V in Table 1), as well as the $\rho$-vector-tensor ($\rho$-VT) coupling and the time component of $\rho$-tensor ($\rho$-T) one in PKA1, introduce new couplings between the $U$- and $L$-components of Dirac spinors, which are repulsive but generally missing in RMF. As seen from the $UL$-F terms in Table 1, these coupling channels further enhance the repulsive $UL$-terms. Therefore from RMF to RHF, the $UL$-terms, as well as the total, become more repulsive for the DIPs $(\nu 2p_{1/2}, \nu s_{1/2})$, seeing Fig. 3. It is worthwhile to mention that different enhancement from PKO3 to PKA1 on the repulsive $UL$-terms in Fig. 3 (b), e.g., for the neutron DIPs $(\nu 2p_{1/2}, \nu 1s_{1/2})$ and $(\nu 2p_{1/2}, \nu 2s_{1/2})$, cannot be simply interpreted by the effects of the additional $\rho$-T and $\rho$-VT couplings, which are due to different in-medium balance between the $\sigma$-S and $\omega$-V couplings between PKA1 and PKO3 as clarified in Ref. [58].

As an implemented test, we performed the calculations with PKA1 for $^{54}$Ca, in which the repulsive $UL$-terms felt by the neutron $s$-orbits from their neutron DIP $\nu 2p_{1/2}$ are dropped, and the results are shown in the last row of Fig. 2 (marked as $^{54}$Ca$^\star$). Similar as $^{52}$Ca, the central-bumped structures appear in both neutron and proton densities, and consistently the $\nu 2p$ splitting becomes large enough to artificially give the $N = 32$ subshell and eliminate the $N = 34$ one. Combined with Figs. 2 and 3, it is clear that the valence neutrons occupying the $\nu 2p_{1/2}$ orbit, via the repulsive couplings with its neutron DIPs $\nu s_{1/2}$, lead to the dramatic changes of the central densities, which is essential for the emergence of the prominent $N = 34$ subshell in $^{54}$Ca.

As indicated from Fig. 3, the $UL$-terms of the DIPs’ couplings, here the doublets $(s_{1/2}, \nu 2p_{1/2})$, are largely enhanced, compared to the others, e.g., the $(s_{1/2}, \nu 2p_{3/2})$ couplings. It is thus appealing to further study the effects in opening the $N = 32$ subshell of $^{52}$Ca, i.e., the $\nu 2p$ splitting $\Delta E_{\nu 2p}$. Fig. 4 (a) shows the evolution of $\Delta E_{\nu 2p}$ values (MeV) from $^{54}$Ca to $^{52}$Ca and further from $^{52}$Ca to $^{46}$Si along the isotonic chain of $N = 32$, as well as the contributions from the $(s_{1/2}, \nu 2p)$ couplings $V_{s_{1/2},\nu 2p}$ (in open circles) and their $UL$-terms (in central-dotted circles). It is seen that the $\Delta E_{\nu 2p}$ values given by PKA1 climb up from $^{54}$Ca to $^{52}$Ca, remain stable from

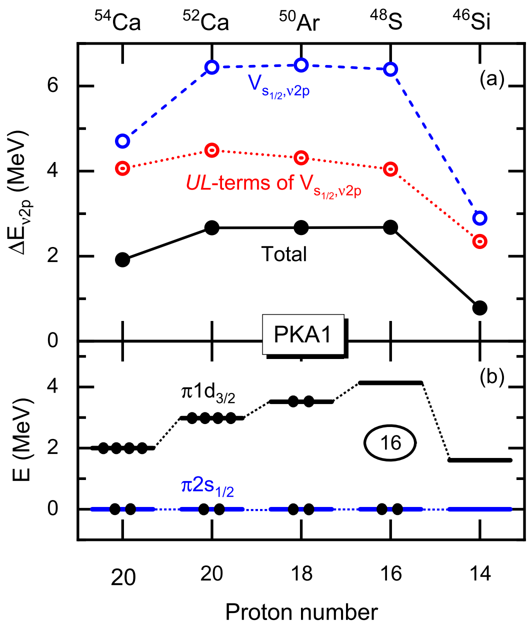


**Fig. 4.** Plot (a) shows the total SO splitting of $\nu 2p$ states (in filled circles), as well as the contributions from the $(s_{1/2}, \nu 2p)$ couplings $V_{s_{1/2},\nu 2p}$ (in open circles) and their $UL$-terms (in central-dotted circles), from $^{54}$Ca to $^{52}$Ca and further from $^{52}$Ca to $^{46}$Si along the isotonic chain of $N = 32$. Schematically, plot (b) shows the proton orbits $\pi 2s_{1/2}$ and $\pi 1d_{3/2}$, in which the black circles denote the protons occupying the orbits. The results are calculated by PKA1.

$^{52}$Ca to $^{48}$S, and suddenly drop in $^{46}$Si. Specifically, the $s$-orbits, the DIPs of $\nu 2p_{1/2}$, present notable contribution to the $\nu 2p$ splittings, mainly from the $UL$-terms which almost fully describe the evolution.

In fact, such systematics are essentially determined by the variations of $s$-orbits, the DIPs of $\nu 2p_{1/2}$. As mentioned before, the presence of repulsive neutron DIPs $(\nu s_{1/2}, \nu 2p_{1/2})$ couplings in $^{54}$Ca, due to the repulsive $UL$-terms, reduces the central probability densities of $s$-orbits, triggering the dramatic density evolution from $^{52}$Ca to $^{54}$Ca, seeing Figs. 2 and 3. From Fig. 4 (b), the proton spectra of $^{54}$Ca ($N = 34$) and the selected $N = 32$ isotones, it is seen that PKA1 presents notable subshell gap $Z = 16$, particularly in $^{48}$S, which stabilizes the full occupation on the proton $\pi 2s_{1/2}$ orbit in $^{50}$Ar and $^{48}$S. Such that the non-vanishing strong coupling between the DIPs $(\pi 2s_{1/2}, \nu 2p_{1/2})$ ensures the persistency of the magicity $N = 32$ in these two isotones, being consistent with the experimentally revealed magicity $N = 32$ in $^{50}$Ar [16]. Further to $^{46}$Si, the empty $\pi 2s_{1/2}$ orbit leads to the vanishing of the strong interaction between the DIPs $(\pi 2s_{1/2}, \nu 2p_{1/2})$. As a result, the largely reduced $\nu 2p$ splitting eliminates the $N = 32$ subshell, seeing Fig. 4 (a). Thus, $^{48}$S is predicted to be the last even isotone that possesses the magicity $N = 32$ on the proton-deficient side ($Z \leqslant 20$), and also a doubly magic nucleus.

Different from $^{54}$Ca, the central-depressed proton density profile appearing in $^{46}$Si, being consistent with the reduced $\nu 2p$ splitting, is due to the empty $\pi 2s_{1/2}$ orbit. Combined with the results in Figs. 2 and 3, it can be seen that either the emergence of new magicity $N = 34$ in $^{54}$Ca or the persistence of the $N = 32$ subshell from $^{52}$Ca to $^{48}$S, as well as its quenching in $^{46}$Si, can be originally due to the presence/vanishing of the strong couplings between the DIPs $(s_{1/2}, \nu 2p_{1/2})$. Consistently, the central density profiles can be essentially changed not only by the reduced occupations of $s$-orbits from $^{48}$S to $^{46}$Si, but also by the reduced central probability density distributions of $s$-orbits from $^{52}$Ca to $^{54}$Ca, and so do the $\nu 2p$ splittings.

In conclusion, the continuous magic nature at $N = 32$ and 34 in Ca isotopes are illustrated by using the relativistic Hartree-Fock (RHF) Lagrangian PKA1 as referred to recent experiments. It is shown that large spin-orbit (SO) splitting of $\nu$2p orbits presents the subshell at $N = 32$ in $^{52}$Ca, whereas significantly reduced $\nu$2p splitting, together with nearly unchanged $\nu$1f one, leads to the magicity $N = 34$ in $^{54}$Ca. Such essential changes of the $\nu$2p splitting can be interpreted self-consistently, following the density evolution from central-bumped structures in $^{52}$Ca to the central-flat (proton) and even central-depressed (neutron) ones in $^{54}$Ca. Moreover, it is found that the dramatic density evolution originates from the strong repulsive interaction between the "Dirac inversion partners" (DIPs) $(\nu 2p_{1/2}, \nu s_{1/2})$. Finally, we also reveal the mechanism for the appearance of new magicity $N = 32$, by analyzing the significant role played by $s_{1/2}$ orbits, which determines the SO spitting of $\nu 2p$ orbits through the strong couplings with the DIP $\nu 2p_{1/2}$. As a result, $^{48}$S is predicted to be the last even isotone preserving the magicity $N = 32$ on the proton-deficient side, and together with the predicted proton subshell $Z = 16$, it can be also a doubly magic nucleus.

## Declaration of competing interest

The authors declare that they have no known competing financial interests or personal relationships that could have appeared to influence the work reported in this paper.

## Acknowledgement

This work is partly supported by the Strategic Priority Research Program of Chinese Academy of Sciences, Grant No. XDB34000000, and Fundamental Research Funds for the Central Universities under Grant No. lzujbky-2019-11, and the National Natural Science Foundation of China under Grant Nos. 11675065 and 11875152. The authors also want to thank Prof. Peter Ring, Prof. Jie Meng and Dr. Pengwei Zhao for fruitful discussions, and the Supercomputer Center of HIRFL for the computation resources.

## References

[1] M.G. Mayer, On closed shells in nuclei, Phys. Rev. 74 (1948) 235–239.
[2] O. Haxel, J.H.D. Jensen, H.E. Suess, On the "Magic Numbers" in nuclear structure, Phys. Rev. 75 (1949) 1766.
[3] T. Otsuka, R. Fujimoto, Y. Utsuno, B.A. Brown, M. Honma, T. Mizusaki, Magic numbers in exotic nuclei and spin-isospin properties of the NN interaction, Phys. Rev. Lett. 87 (2001) 082502.
[4] J. Meng, H. Toki, S.G. Zhou, S.Q. Zhang, W.H. Long, L.S. Geng, Relativistic continuum Hartree-Bogoliubov theory for the ground state properties of exotic nuclei, Prog. Part. Nucl. Phys. 57 (2006) 470–563.
[5] H. Simon, D. Aleksandrov, T. Aumann, L. Axelsson, T. Baumann, M.J.G. Borge, L.V. Chulkov, R. Collatz, J. Cub, W. Dostal, Direct experimental evidence for strong admixture of different parity states in $^{11}$Li, Phys. Rev. Lett. 83 (1999) 496–499.
[6] T. Motobayashi, Y. Ikeda, K. Ieki, M. Inoue, N. Iwasa, T. Kikuchi, M. Kurokawa, S. Moriya, S. Ogawa, H. Murakami, S. Shimoura, Y. Yanagisawa, T. Nakamura, Y. Watanabe, M. Ishihara, T. Teranishi, H. Okuno, R.F. Casten, Large deformation of the very neutron-rich nucleus $^{32}$Mg from intermediate-energy Coulomb excitation, Phys. Lett. B 346 (1995) 9–14.
[7] A. Ozawa, T. Kobayashi, T. Suzuki, K. Yoshida, I. Tanihata, New magic number, N = 16, near the neutron drip-line, Phys. Rev. Lett. 84 (2000) 5493–5495.
[8] C.R. Hoffman, T. Baumann, D. Bazin, J. Brown, G. Christian, et al., Determination of the $N = 16$ shell closure at the oxygen drip line, Phys. Rev. Lett. 100 (2008) 152502.
[9] R. Kanungo, C. Nociforo, A. Prochazka, T. Aumann, D. Boutin, D. Cortina-Gil, B. Davids, M. Diakaki, F. Farinon, H. Geissel, R. Gernhäuser, J. Gerl, R. Janik, B. Jonson, B. Kindler, R. Knöbel, R. Krücken, M. Lantz, H. Lenske, Y. Litvinov, B. Lommel, K. Mahata, P. Maierbeck, A. Musumarra, T. Nilsson, T. Otsuka, C. Perro, C. Scheidenberger, B. Sitar, P. Strmen, B. Sun, I. Szarka, I. Tanihata, Y. Utsuno, One-neutron removal measurement reveals $^{24}$O as a new doubly magic nucleus, Phys. Rev. Lett. 102 (2009) 152501.
[10] K. Tshoo, Y. Satou, H. Bhang, S. Choi, T. Nakamura, Y. Kondo, S. Deguchi, Y. Kawada, N. Kobayashi, Y. Nakayama, K.N. Tanaka, N. Tanaka, N. Aoi, M. Ishihara, T. Motobayashi, H. Otsu, H. Sakurai, S. Takeuchi, Y. Togano, K. Yoneda, Z.H. Li, F. Delaunay, J. Gibelin, F.M. Marqués, N.A. Orr, T. Honda, M. Matsushita,

T. Kobayashi, Y. Miyashita, T. Sumikama, K. Yoshinaga, S. Shimoura, D. Sohler, T. Zheng, Z.X. Cao, $N = 16$ spherical shell closure in $^{24}$O, Phys. Rev. Lett. 109 (2012) 022501.

[11] I. Tanihata, H. Savajols, R. Kanungo, Recent experimental progress in nuclear halo structure studies, Prog. Part. Nucl. Phys. 68 (2013) 215–313.

[12] J.I. Prisciandaro, P.F. Mantica, B.A. Brown, D.W. Anthony, M.W. Cooper, A. Garcia, D.E. Groh, A. Komives, W. Kumarasiri, P.A. Lofy, New evidence for a subshell gap at $N = 32$, Phys. Lett. B 510 (2001) 17–23.

[13] R.V.F. Janssens, B. Fornal, P.F. Mantica, B.A. Brown, R. Broda, P. Bhattacharyya, M.P. Carpenter, M. Cinausero, P.J. Daly, A.D. Davies, T. Glasmacher, Z.W. Grabowski, D.E. Groh, M. Honma, F.G. Kondev, W. Królas, T. Lauritsen, S.N. Liddick, S. Lunardi, N. Marginean, T. Mizusaki, D.J. Morrissey, A.C. Morton, W.F. Mueller, T. Otsuka, T. Pawlat, D. Seweryniak, H. Schatz, A. Stolz, S.L. Tabor, C.A. Ur, G. Viesti, I. Wiedenhöver, J. Wrzesiński, Structure of $^{52,54}$Ti and shell closures in neutron-rich nuclei above $^{48}$Ca, Phys. Lett. B 546 (2002) 55–62.

[14] D.C. Dinca, R.V.F. Janssens, A. Gade, D. Bazin, R. Broda, B.A. Brown, C.M. Campbell, M.P. Carpenter, P. Chowdhury, J.M. Cook, A.N. Deacon, B. Fornal, S.J. Freeman, T. Glasmacher, M. Honma, F.G. Kondev, J.L. Lecouey, S.N. Liddick, P.F. Mantica, W.F. Mueller, H. Olliver, T. Otsuka, J.R. Terry, B.A. Tomlin, K. Yoneda, Reduced transition probabilities to the first $2^+$ state in $^{52,54,56}$Ti and development of shell closures at $N = 32, 34$, Phys. Rev. C 71 (2005) 041302.

[15] A. Gade, R.V.F. Janssens, D. Bazin, R. Broda, B.A. Brown, C.M. Campbell, M.P. Carpenter, J.M. Cook, A.N. Deacon, D.-C. Dinca, B. Fornal, S.J. Freeman, T. Glasmacher, P.G. Hansen, B.P. Kay, P.F. Mantica, W.F. Mueller, J.R. Terry, J.A. Tostevin, S. Zhu, Cross-shell excitation in two-proton knockout: structure of $^{52}$Ca, Phys. Rev. C 74 (2006) 021302(R).

[16] D. Steppenbeck, S. Takeuchi, N. Aoi, P. Doornenbal, M. Matsushita, H. Wang, Y. Utsuno, H. Baba, S. Go, J. Lee, K. Matsui, S. Michimasa, T. Motobayashi, D. Nishimura, T. Otsuka, H. Sakurai, Y. Shiga, N. Shimizu, P.-A. Söderström, T. Sumikama, R. Taniuchi, J.J. Valiente-Dobón, K. Yoneda, Low-lying structure of $^{50}$Ar and the $N = 32$ subshell closure, Phys. Rev. Lett. 114 (2015) 252501.

[17] F. Wienholtz, D. Beck, K. Blaum, C. Borgmann, M. Breitenfeldt, R.B. Cakirli, S. George, F. Herfurth, J.D. Holt, M. Kowalska, S. Kreim, D. Lunney, V. Manea, J. Menendez, D. Neidherr, M. Rosenbusch, L. Schweikhard, A. Schwenk, J. Simonis, J. Stanja, R.N. Wolf, K. Zuber, Masses of exotic calcium isotopes pin down nuclear forces, Nature 498 (2013) 346–349.

[18] A.T. Gallant, J.C. Bale, T. Brunner, U. Chowdhury, S. Ettenauer, A. Lennarz, D. Robertson, V.V. Simon, A. Chaudhuri, J.D. Holt, A.A. Kwiatkowski, E. Mane, J. Menendez, B.E. Schultz, M.C. Simon, C. Andreoiu, P. Delheij, M.R. Pearson, H. Savajols, A. Schwenk, J. Dilling, New precision mass measurements of neutron-rich calcium and potassium isotopes and three-nucleon forces, Phys. Rev. Lett. 109 (2012) 032506.

[19] M. Rosenbusch, P. Ascher, D. Atanasov, C. Barbieri, D. Beck, K. Blaum, C. Borgmann, M. Breitenfeldt, R.B. Cakirli, A. Cipollone, S. George, F. Herfurth, M. Kowalska, S. Kreim, D. Lunney, V. Manea, P. Navratil, D. Neidherr, L. Schweikhard, V. Soma, J. Stanja, F. Wienholtz, R.N. Wolf, K. Zuber, Probing the $N = 32$ shell closure below the magic proton number $Z = 20$: mass measurements of the exotic isotopes $^{52,53}$K, Phys. Rev. Lett. 114 (2015) 202501.

[20] X. Xu, M. Wang, K. Blaum, J.D. Holt, Y.A. Litvinov, A. Schwenk, J. Simonis, S.R. Stroberg, Y.H. Zhang, H.S. Xu, P. Shuai, X.L. Tu, X.H. Zhou, F.R. Xu, G. Audi, R.J. Chen, X.C. Chen, C.Y. Fu, Z. Ge, W.J. Huang, S. Litvinov, D.W. Liu, Y.H. Lam, X.W. Ma, R.S. Mao, A. Ozawa, B.H. Sun, Y. Sun, T. Uesaka, G.Q. Xiao, Y.M. Xing, T. Yamaguchi, Y. Yamaguchi, X.L. Yan, Q. Zeng, H.W. Zhao, T.C. Zhao, W. Zhang, W.L. Zhan, Masses of neutron-rich $^{52-54}$Sc and $^{54,56}$Ti nuclides: the $N = 32$ subshell closure in scandium, Phys. Rev. C 99 (2019) 064303.

[21] M.P. Reiter, S.A.S. Andres, E. Dunling, B. Koote, E. Leistenschneider, C. Andreoiu, C. Babcock, B.R. Barquest, J. Bollig, T. Brunner, I. Dillmann, A. Finlay, G. Gwinner, L. Graham, J.D. Holt, C. Hornung, C. Jesch, R. Klawitter, Y. Lan, D. Lascar, J.E. McKay, S.F. Paul, R. Steinbrugge, R. Thompson, J.L. Tracy, M.E. Wieser, C. Will, T. Dickel, W.R. Plaß, C. Scheidenberger, A.A. Kwiatkowski, J. Dilling, Quenching of the $N = 32$ neutron shell closure studied via precision mass measurements of neutron-rich vanadium isotopes, Phys. Rev. C 98 (2018) 024310.

[22] D. Steppenbeck, S. Takeuchi, N. Aoi, P. Doornenbal, M. Matsushita, H. Wang, H. Baba, N. Fukuda, S. Go, M. Honma, J. Lee, K. Matsui, S. Michimasa, T. Motobayashi, D. Nishimura, T. Otsuka, H. Sakurai, Y. Shiga, P.A. Soderstrom, T. Sumikama, H. Suzuki, R. Taniuchi, Y. Utsuno, J.J. Valiente-Dobon, K. Yoneda, Evidence for a new nuclear 'magic number' from the level structure of $^{54}$Ca, Nature 502 (2013) 207–210.

[23] S.N. Liddick, P.F. Mantica, R.V.F. Janssens, R. Broda, B.A. Brown, et al., Lowest excitations in $^{56}$Ti and the predicted $N = 34$ shell closure, Phys. Rev. Lett. 92 (2004) 072502.

[24] T.R. Rodriguez, J.L. Egido, New beyond-mean-field theories: examination of the potential shell closures at $N = 32$ or 34, Phys. Rev. Lett. 99 (2007) 062501.

[25] G. Hagen, M. Hjorth-Jensen, G.R. Jansen, R. Machleidt, T. Papenbrock, Evolution of shell structure in neutron-rich calcium isotopes, Phys. Rev. Lett. 109 (2012) 032502.

[26] M. Honma, T. Otsuka, B.A. Brown, T. Mizusaki, Shell-model description of neutron-rich $pf$-shell nuclei with a new effective interaction GXPF1, Eur. Phys. J. A 25 (2005) 499–502.

[27] H. Hergert, S.K. Bogner, T.D. Morris, S. Binder, A. Calci, J. Langhammer, R. Roth, Ab initio multireference in-medium similarity renormalization group calculations of even calcium and nickel isotopes, Phys. Rev. C 90 (2014) 041302(R).

[28] S. Michimasa, M. Kobayashi, Y. Kiyokawa, S. Ota, D.S. Ahn, H. Baba, G.P.A. Berg, M. Dozono, N. Fukuda, T. Furuno, E. Ideguchi, N. Inabe, T. Kawabata, S. Kawase, K. Kisamori, K. Kobayashi, T. Kubo, Y. Kubota, C.S. Lee, M. Matsushita, H. Miya, A. Mizukami, H. Nagakura, D. Nishimura, H. Oikawa, H. Sakai, Y. Shimizu, A. Stolz, H. Suzuki, M. Takaki, H. Takeda, S. Takeuchi, H. Tokieda, T. Uesaka, K. Yako, Y. Yamaguchi, Y. Yanagisawa, R. Yokoyama, K. Yoshida, S. Shimoura, Magic nature of neutrons in $^{54}$Ca: first mass measurements of $^{55-57}$Ca, Phys. Rev. Lett. 121 (2018) 022506.

[29] H.N. Liu, A. Obertelli, P. Doornenbal, C.A. Bertulani, G. Hagen, J.D. Holt, G.R. Jansen, T.D. Morris, A. Schwenk, R. Stroberg, N. Achouri, H. Baba, F. Browne, D. Calvet, F. Château, S. Chen, N. Chiga, A. Corsi, M.L. Cortés, A. Delbart, J.-M. Gheller, A. Giganon, A. Gillibert, C. Hilaire, T. Isobe, T. Kobayashi, Y. Kubota, V. Lapoux, T. Motobayashi, I. Murray, H. Otsu, V. Panin, N. Paul, W. Rodriguez, H. Sakurai, M. Sasano, D. Steppenbeck, L. Stuhl, Y.L. Sun, Y. Togano, T. Uesaka, K. Wimmer, K. Yoneda, O. Aktas, T. Aumann, L.X. Chung, F. Flavigny, S. Franchoo, I. Gašparić, R.-B. Gerst, J. Gibelin, K.I. Hahn, D. Kim, T. Koiwai, Y. Kondo, P. Koseoglou, J. Lee, C. Lehr, B.D. Linh, T. Lokotko, M. MacCormick, K. Moschner, T. Nakamura, S.Y. Park, D. Rossi, E. Sahin, D. Sohler, P.-A. Söderström, S. Takeuchi, H. Törnqvist, V. Vaquero, V. Wagner, S. Wang, V. Werner, X. Xu, H. Yamada, D. Yan, Z. Yang, M. Yasuda, L. Zanetti, How robust is the $N = 34$ subshell closure? first spectroscopy of $^{52}$Ar, Phys. Rev. Lett. 122 (2019) 072502.

[30] J.D. Walecka, A theory of highly condensed matter, Ann. Phys. (N. Y.) 83 (1974) 491–529.

[31] B.D. Serot, J.D. Walecka, The relativistic nuclear many-body problem, Adv. Nucl. Phys. 16 (1986) 1–327.

[32] P. Ring, Relativistic mean field theory in finite nuclei, Prog. Part. Nucl. Phys. 37 (1996) 193–263.

[33] M. Bender, P.-H. Heenen, P.-G. Reinhard, Self-consistent mean-field models for nuclear structure, Rev. Mod. Phys. 75 (2003) 121–180.

[34] D. Vretenar, A.V. Afanasjev, G.A. Lalazissis, P. Ring, Relativistic Hartree-Bogoliubov theory: static and dynamic aspects of exotic nuclear structure, Phys. Rep. 409 (2005) 101–259.

[35] H. Liang, J. Meng, S.-G. Zhou, Hidden pseudospin and spin symmetries and their origins in atomic nuclei, Phys. Rep. 570 (2015) 1–84.

[36] J. Meng (Ed.), Relativistic Density Functional for Nuclear Structure, International Review of Nuclear Physics, vol. 10, World Scientific, Singapore, 2016.

[37] H.Z. Liang, N. Van Giai, J. Meng, Spin-isospin resonances: a self-consistent covariant description, Phys. Rev. Lett. 101 (2008) 122502.

[38] W.H. Long, T. Nakatsukasa, H. Sagawa, J. Meng, H. Nakada, Y. Zhang, Non-local mean field effect on nuclei near sub-shell, Phys. Lett. B 680 (2009) 428–431.

[39] W.H. Long, P. Ring, J. Meng, N. Van Giai, C.A. Bertulani, Nuclear halo structure and pseudospin symmetry, Phys. Rev. C 81 (2010) 031302(R).

[40] J.J. Li, J. Margueron, W.H. Long, N.V. Giai, Magicity of neutron-rich nuclei within relativistic self-consistent approaches, Phys. Lett. B 753 (2016) 97–102.

[41] S. Shen, H. Liang, W.H. Long, J. Meng, P. Ring, Towards an ab initio covariant density functional theory for nuclear structure, Prog. Part. Nucl. Phys. (2019) 103713.

[42] G.A. Lalazissis, T. Nikšić, D. Vretenar, P. Ring, New relativistic mean-field interaction with density-dependent meson-nucleon couplings, Phys. Rev. C 71 (2005) 024312.

[43] P.W. Zhao, Z.P. Li, J.M. Yao, J. Meng, New parametrization for the nuclear covariant energy density functional with a point-coupling interaction, Phys. Rev. C 82 (2010) 054319.

[44] W.H. Long, J. Meng, N.V. Giai, S.-G. Zhou, New effective interactions in RMF theory with non-linear terms and density-dependent meson-nucleon coupling, Phys. Rev. C 69 (2004) 034319.

[45] W.H. Long, N. Van Giai, J. Meng, Density-dependent relativistic Hartree-Fock approach, Phys. Lett. B 640 (2006) 150–154.

[46] W.H. Long, H. Sagawa, J. Meng, N. Van Giai, Evolution of nuclear shell structure due to the pion exchange potential, Europhys. Lett. 82 (2008) 12001.

[47] W.H. Long, H. Sagawa, N. Van Giai, J. Meng, Shell structure and $\rho$-tensor correlations in density dependent relativistic Hartree-Fock theory, Phys. Rev. C 76 (2007) 034314.

[48] L.J. Wang, J.M. Dong, W.H. Long, Tensor effects on the evolution of the $N = 40$ shell gap from nonrelativistic and relativistic mean-field theory, Phys. Rev. C 87 (2013) 047301.

[49] J.F. Berger, M. Girod, D. Gogny, Microscopic analysis of collective dynamics in low energy fission, Nucl. Phys. A 428 (1984) 23–36.

[50] W.H. Long, P. Ring, N.V. Giai, J. Meng, Relativistic Hartree-Fock-Bogoliubov theory with density dependent meson-nucleon couplings, Phys. Rev. C 81 (2010) 024308.

[51] Hartree-Fock-Bogoliubov results based on the Gogny force, http://www-phynu.cea.fr/science_en_ligne/carte_potentiels_microscopiques/carte_potentiel_nucleaire_eng.htm#info.

[52] M. Wang, G. Audi, F.G. Kondev, W.J. Huang, S. Naimi, X. Xu, The AME2016 atomic mass evaluation (II). Tables, graphs and references, Chin. Phys. C 41 (2017) 030003.

[53] W. Satula, J. Dobaczewski, W. Nazarewicz, Odd-even staggering of nuclear mass: pairing or shape effect?, Phys. Rev. Lett. 81 (1998) 3599–3602.
[54] B.G. Todd-Rutel, J. Piekarewicz, P.D. Cottle, Spin-orbit splitting in low-$j$ neutron orbits and proton densities in the nuclear interior, Phys. Rev. C 69 (2004) 021301(R).
[55] G. Burgunder, O. Sorlin, F. Nowacki, S. Giron, F. Hammache, M. Moukaddam, N. de Sereville, D. Beaumel, L. Caceres, E. Clement, G. Duchene, J.P. Ebran, B. Fernandez-Dominguez, F. Flavigny, S. Franchoo, J. Gibelin, A. Gillibert, S. Grevy, J. Guillot, A. Lepailleur, I. Matea, A. Matta, L. Nalpas, A. Obertelli, T. Otsuka, J. Pancin, A. Poves, R. Raabe, J.A. Scarpaci, I. Stefan, C. Stodel, T. Suzuki, J.C. Thomas, Experimental study of the two-body spin-orbit force in nuclei, Phys. Rev. Lett. 112 (2014) 042502.
[56] J.J. Li, W.H. Long, J. Magueron, N.V. Giai, $^{48}$Si: an atypical nucleus?, Phys. Lett. B 788 (2019) 192–197.
[57] T. Otsuka, A. Gade, O. Sorlin, T. Suzuki, Y. Utsuno, Evolution of nuclear structure in exotic nuclei driven by nuclear forces, arXiv:1805.06501, 2018.
[58] J. Geng, J.J. Li, W.H. Long, Y.F. Niu, S.Y. Chang, Pseudospin symmetry restoration and the in-medium balance between nuclear attractive and repulsive interactions, Phys. Rev. C 100 (2019) 051301(R).